Cooled Gas Turbine Blade Trailing Edge Flow Analysis

Márcio Teixeira de Mendonça, marcio@ita.br
Instituto Tecnológico de Aeronáutica, Divisão de Engenharia Mecânica Aeronáutica ITA/IEM
Phone (12) 3947 6951, São José dos Campos, SP, Brazil, CEP 12228-900

Abstract. *The flow on the rotating blades of a turbine is unsteady due to the wake of the stator blade row upstream. This unsteadiness is a source of losses and complex flow structures on the rotor blade due to the variation on the turbulence levels and location of the boundary layer laminar to turbulent transition. Convective cooled blades oftentime have cooling air ejected at the trailing edge right at the blade wake. The present ivestigation presents an analysis of a canonical flow consistent with the flow topology found at the trailing edge of a gas turbine blade with coolant ejection. A hydrodynamic stability analysis is performed for the combined wake and jet velocity profiles given by a gaussian distribution representing the turbulent rms wake and a laminar jet superposed. The growth rate of any instability found on the flow is an indication of faster mixing, resulting in a reduction on the wake velocity defect and consequently on the complexity associated with it. The results show that increasing the Mach number or the three-dimensionality of the disturbiances result in a reduction of the amplification rate. When the flow at the trailing edge is modified by a jet, the amplification rates are lower, but the range of unstable streamwise wavenumbers is larger.*

Keywords: *gas turbine cooling, gas turbine losses, hydrodynamic stability analysis*

1. INTRODUCTION

Gas turbine efficiency, specific thrust and specific fuel consumption can be improved increasing the turbine entry temperature (TET) and compressor pressure ratio. Due to metallurgical considerations, in order to use the highest possible TET the stator and rotor blades have to be cooled. The cooling system introduces losses associated with the interference between the combustion gases on the main stream and the cooling flow, which is ejected on the blade surface in film cooling or ejected through the trailing edge in convection cooling.

In order to further improve gas turbine blade cooling systems and reduce losses a stronger physical understanding of the flow and heat transfer processes are mandatory. The present investigation considers the trailing edge cooling flow ejection into the main stream and the resulting interference between the cooling jet and the main flow wake. The analysis is restricted to the early stages of transition of the laminar cooling jet exposed to the turbulent shear layer just down stream of the trailing edge. Nevertheless, the large tubulent structures downstream on the wake region are originated on the instabilities (Winant and Browand, 1974; Brown and Roshko, 1974).

The parameters considered are the jet to main stream velocity ratio, Mach number, jet to wake thickness ratio and disturbance three-dimensionality given by the spanwise wavelength. This three dimensional effects are relevant to establish the spanwise distribution of cooling holes on gill and letter box trailing edge configurations.

Enhancing the mixing of the laminar trailing edge jet with the main stream wake will result in a positive reduction on the wake defect. In other words, energizing the wake with the cooling flow reduces the unsteadiness in subsequent blade rows. This mixing will be stronger the stronger the instabilities in the laminar trailing edge jet. To gain further understanding on the mixing process a laminar flow stability analysis is performed using a local, normal modes approach and a search is performed to identify the conditions that maximize the growth rate and maximize the range of unstable frequencies and wavenumbers. The stronger the instability modes are, the faster the mixing between the mains stream and the cooling jet.

The literature has a considerable amount of studies dedicated to the stability of mixing layers, both for compressible and incompressible flows, considering either a single species or binary systems (Ho and Huerre, 1984; Fedioun and Lardjane, 2005; Salemi and Mendonca, 2008; Caillol, 2009) (and references therein). But, in engineering application it is not uncommon to have shear layers modified by a wake or a combination of a mixing layer, a wake and a jet, such as the case under analysis.

The combined effect of a wake and a compressible mixing layer was investigate by Zhuang (1995). They found that the mixing layer becomes more unstable with increasing wake deficit and that compressibility has a stabilizing effect on the wake.

The effect of an asymmetric wave profile, which is composed of a mixing layer and a wake, has also been investigated by Gennaro and Medeiros (2008). Their investigation for incompressible flows found that the asymmetric wave has lower ampoification rates and unstable range of wave numbers. The Strouhal number decreases with invreasing asymmetry. The proper scaling factor for the mixing layer modified by a wake has been propose in their work in order to unify results found in previous work.

The effect of a jet on the development of compressible shear layers was investigated by King and Schetz (1996) aiming at the conditions that allow a mixing enhancement. The right combination of shear layer to jet thickness ratio, jet

placement with respect to the shear layer and mixing layer confinement significantly increase growth rates.

2. FORMULATION

The compressible version of the Rayleigh equation for stability analysis is used to calculate stability diagrams where growth rates are obtained for different spanwise and streamwise wave numbers. A Gaussian profile is considered to represent the trailing edge boundary layer $U(\eta)$ wake and jet profiles. Temperature distributions $T(\eta)$ are given by the Crocco-Busemann relation (White, 1974).

2.1 Base Flow

The base flow used for the local stability analysis is given by The canonical gaussian deffect profile for the wake and jet as shown in Eqs. 1 and 2. The wake to jet thickness ratio is n.

$$U_{\text{wake}} = 0.5\left(1 - \tanh^2(\eta)\right) \tag{1}$$

$$U_{\text{jet}} = 0.25\left(1 - \tanh^2(n\eta)\right) \tag{2}$$

The local temperature distribution is given by the Crocco-Busemann relation (Eq. 3), valid for Prandtl number $Pr = 1$ and Chapman-Rubesin paramenter $\mathcal{C} = 1$.

Figure 1 shows the base velocity distribution for the wake and jet.

$$T = 1 + Ma^2 \frac{\gamma - 1.}{2}\left(1 - U_\infty^2\right) \tag{3}$$

Where Ma is the Mach number in the freestream, γ is the ratio of specific heats and U is the freestream velocity.

The base flow topology is presented in Fig. 1 that shows the jet and wake individually and the combined jet plus wake base flow.

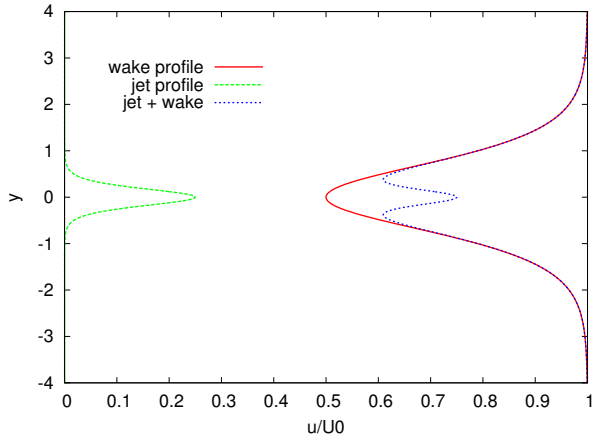

Figure 1. Base canonical flow composed of a jet and a wake profiles.

2.2 Stability Equation

The derivation of the inviscid stability equations are detailed in Salemi and Mendonca (2008). Starting from the Euler equations for an inviscid flow and the perfect gas law, the instantaneos flow is decomposed into a base flow and a small disturbance. A normal mode solution is proposed such that for the disturbances

$$u'(x, y, z, t) = \Re\left\{\hat{u}(y)\exp\left[i\left(\alpha x + \beta z - \omega t\right)\right]\right\} \tag{4}$$

and similarly for the other variables. In the proposed model $\hat{u}$ is the eigenfunction and the eigenvalues α, β and ω are the wavenumbers in the streamwise and spanwise directions and the frequency respectively. For spatial stability analysis α is considered complex and ω real, while for temporal stability analysis α is real and ω complex.

Substituting the proposed normal modes solution on the Euler equations, linearizing and manipulating, results:

$$\hat{\rho}\, i\left(\alpha\bar{u} - \omega\right) + \hat{v}\,\frac{d\bar{\rho}}{dy} + \bar{\rho}\left[i\left(\alpha\hat{u} + \beta\hat{w}\right) + \frac{d\hat{v}}{dy}\right] = 0, \qquad \bar{\rho}\left[i\left(\alpha\bar{u} - \omega\right)\hat{u} + \hat{v}\,\frac{d\bar{u}}{dy}\right] = -\frac{i\alpha\hat{p}}{\gamma_1\, Ma_1^2}, \tag{5}$$

$$\bar{\rho}\, i\,(\alpha\bar{u}-\omega)\,\hat{v} = -\,\frac{1}{\gamma_1\, Ma_1^2}\,\frac{d\hat{p}}{dy}\,, \qquad \bar{\rho}\, i\,(\alpha\bar{u}-\omega)\,\hat{w} = -\,\frac{i\beta\hat{p}}{\gamma_1\, Ma_1^2}\,, \tag{6}$$

$$\bar{\rho}\left[i\,(\alpha\bar{u}-\omega)\,\widehat{T} + \hat{v}\,\frac{d\overline{T}}{dy}\right] = -\,\frac{(\gamma-1)}{R}\left[i\,(\alpha\hat{u}+\beta\hat{w}) + \frac{d\hat{v}}{dy}\right]\,, \tag{7}$$

$$\bar{\rho}\left[i\,(\alpha\bar{u}-\omega)\,\widehat{Y}_1 + \hat{v}\,\frac{d\overline{Y}_1}{dy}\right] = 0\,, \qquad \hat{p} = \bar{\rho}\,R\,\widehat{T} + \hat{\rho}\,R\,\overline{T}\,. \tag{8}$$

With the aid of the transformation introduced by Gropengiesser (1970) given by the χ function, the stability equations can be condensed into only a single ordinary differential equation:

$$\chi = \frac{i\alpha\hat{p}}{\gamma_1\, Ma_1^2\,\hat{v}}, \qquad \frac{d\chi}{dy} = \frac{\alpha^2\,(\bar{u}-\omega/\alpha)}{R\overline{T}} - \chi\left[\frac{\chi G + (d\bar{u}/dy)}{(\bar{u}-\omega/\alpha)}\right], \tag{9}$$

with the following boundary condition:

$$\chi\,(y\to\pm\infty) = \mp\,\frac{\alpha\,(\bar{u}-\omega/\alpha)}{\sqrt{G\,R\,\overline{T}}}\,, \qquad G = \frac{\alpha^2+\beta^2}{\bar{\rho}\,\alpha^2} - Ma_1^2\,\frac{\gamma_1}{\gamma}\,\frac{(\alpha\bar{u}-\omega)^2}{\alpha^2}\,. \tag{10}$$

The resulting eigenvalue problem for the dispersion relation $f(\alpha,\beta,\omega)=0$ posed by the stability equations is solved using a shooting method described in Salemi and Mendonca (2008).

3. RESULTS

First, results are presented in Fig. 2 to 4, where the effect of jet to wake deficit velocity ratio on the amplification factor, wavenumber and phase velocity are considered. The results show that the stronger the trailing edge jet, the stronger the maximum temporal growth rates with an increase of more than two fold when the velocity ratio go from 0.1 to 0.5. The range of unstable frequencies also increase significantly with higher velocity ratios. The phase velocity is relativelly independent of frequency for frequencies above $\omega = 0.4$, which indicate a non-dispersive wave system.

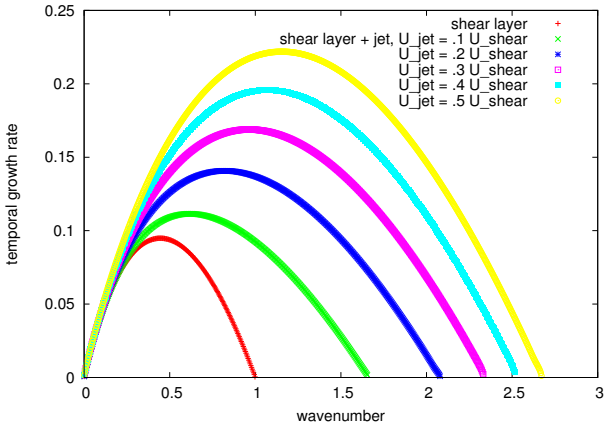

Figure 2. Growth rate as a function of wavenumber, variation with jet to wake velocity ratio.

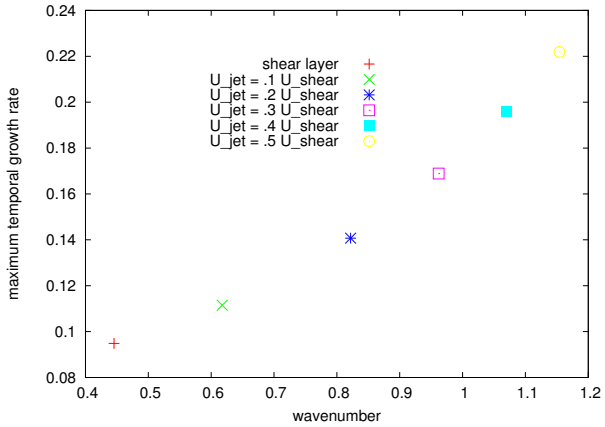

Figure 3. Maximum growth rate variation with jet to wake velocity ratio.

The following results consider comparisons between a wake profile when the upper and lower streams have different freestream velocities such that a mixing layer profile is superimposed on the wake. The stability of this base flow is compared to the stability of the same profile when a jet profile is also superimposed, showing the effect of the jet on this canonical trailing edge wake/mixing layer profile. The individual distribution of jet, wake and mixing layer base laminar velocities and the resulting superpositon for the wake and mixing layer and wake, mixing layer and jet are presented in Fig. 5. The jet to wake deficit velocity ratio is imposed 0.5.

Comparisos are presented for four different Mach numbers at the fast stream, the incompressible regime $Ma = 0$, and three compressible regimes, $Ma = 0.4$, $Ma = 0.8$ and $Ma = 1.2$. Six different propagation angles are defined by the following spanwise wavenumbers β: 0.0, 0.025, 0.05, 0.145, 0.335 and 0.692.

Initially only the wake/mixing layer profile is considered. Figures 6 through 11 show the effect of Mach number for a given spanwise wavenumber. Compressibility effects are stronger for Mach numbers above 0.4. The compressibility has a stabilizing effect on the amplification rate.

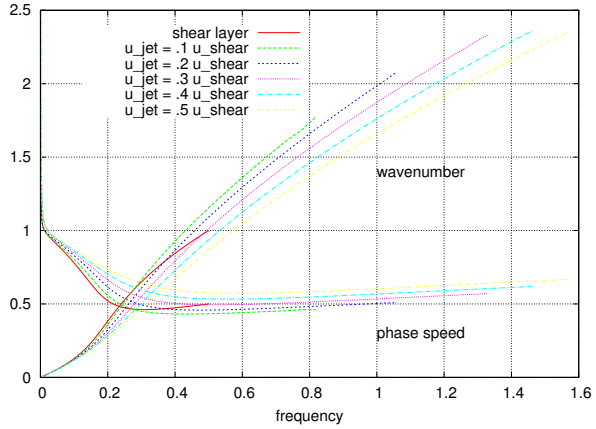

Figure 4. Variation of wavenumber and phase speed with frequency for different velocity ratios.

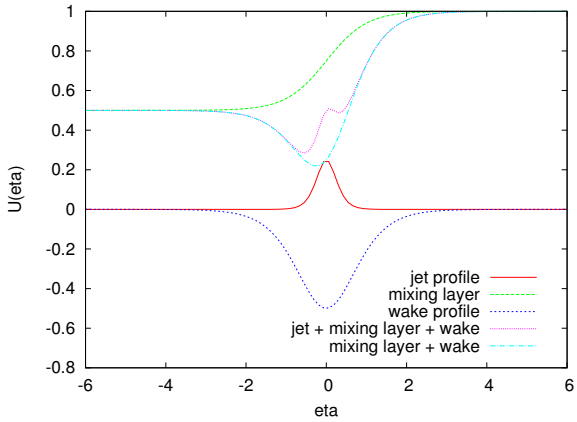

Figure 5. Mean flow velocity profile for a wake and a mixing layer and for a wake, a mixing layer and a jet.

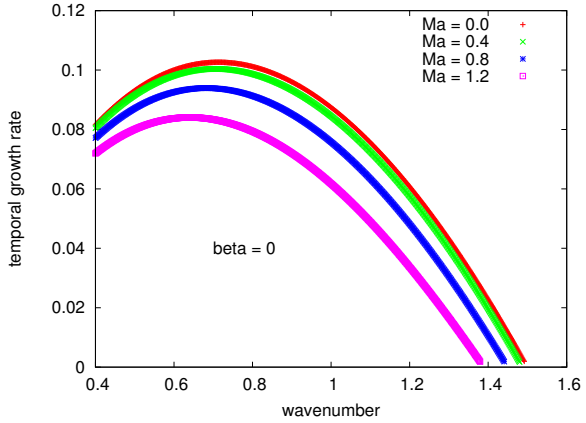

Figure 6. Wavenumber versus growth rate for $\beta = 0.0$

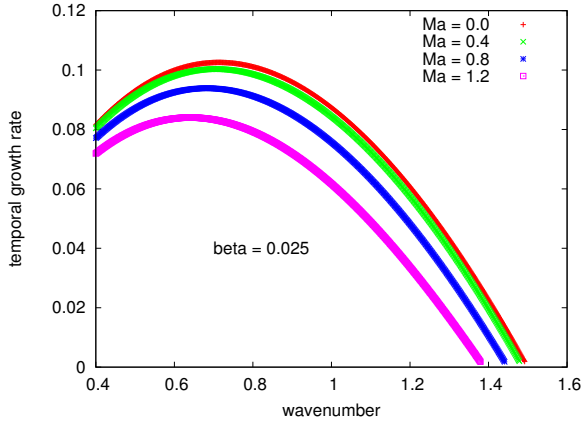

Figure 7. Wavenumber versus growth rate for $\beta = 0.025$

The same results are presented comparing the effect of spanwise wavenumber β for a given Mach number Ma. The most significant effects are found for β above 0.145, where the growth rate decrease with increasing β. Nontheless, the spanwise wavenumber does not change the streamwise wavenumber corresponding to the fastest growth rate.

Next the effect of spanwise wavenumber and Mach number are considered for the based flow composed of a mixing layer, a wake and a jet. Again, four different Mach numbers Ma are considered, 0.0, 0.4, 0.8 and 1.2. And six different spanwise wavenumbers β are considered, 0.0, 0.025, 0.050, 0.145, 0.335 and 0.692.

The results for different spanwise wavenumber are presented in Fig. 16 through 21 showing the effect of Mach number for a given spanwise wavenumber. The growth rate decrease with increasing Mach number as before.

The same results are grouped to show the effect of β for a given Mach number. The results are presented in Fig. 22 through 25 and show the same trends found for the wake/mixing layer profile with decreasing growth rate with increasing spanwise wave number.

Figures 26 through 29 show comparisons between the trailing edge flow with and without jet for the four Mach numbers considered. When a jet is present in the trailing edge flow there is a reduction on the maximum growth rate and an increase on the range of unstable wavenumbers. The behaviour with varying Mach number and spanwise wavenumber is very similar for the cases when the jet is not present presented previously. The most significant feature of these results is that, while the effect of the jet on the wake is destabilizing, the effect of the jet on the wake/mixing layer profile is stabilizing.

Figure 30 show the variation of the phase speed with spanwise wavenumber for $Ma = 1.2$. Unlike the results for the interaction of a wake and a jet, when a mixing layer is also present the wave system is dispersive. The interesting result is that the phase speed vary little with the spanwise wavenumber. Likewise, the phase speed does not depende strongly on the Mach number as presented in Fig. 31 for $\beta = 0.145$. Similar results are obtained for other Mach numbers and spanwise wavenumbers.

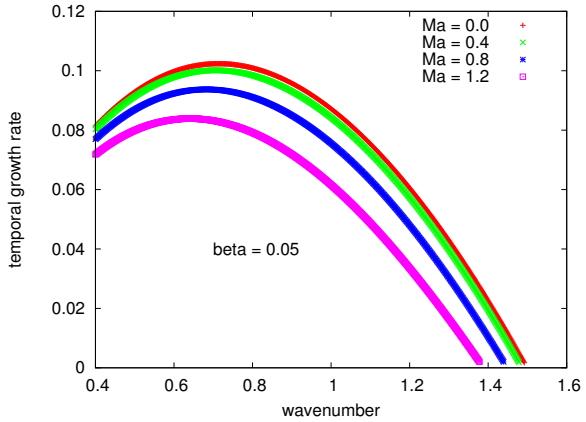

Figure 8. Wavenumber versus growth rate for $\beta = 0.05$

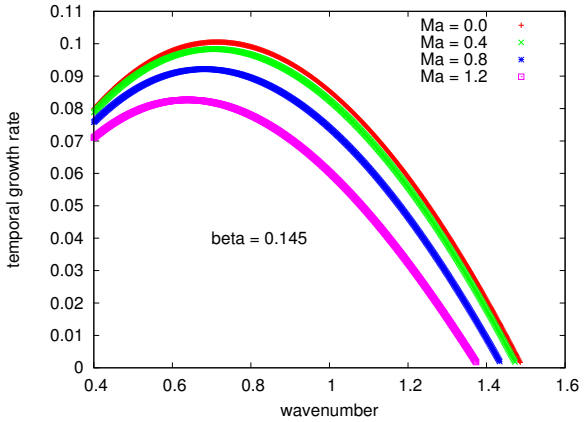

Figure 9. Wavenumber versus growth rate for $\beta = 0.145$

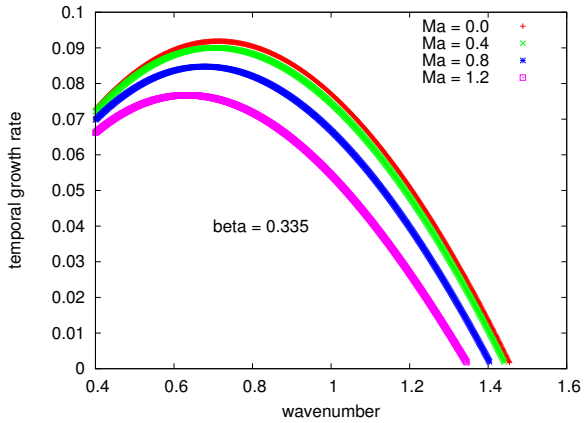

Figure 10. Wavenumber versus growth rate for $\beta = 0.335$

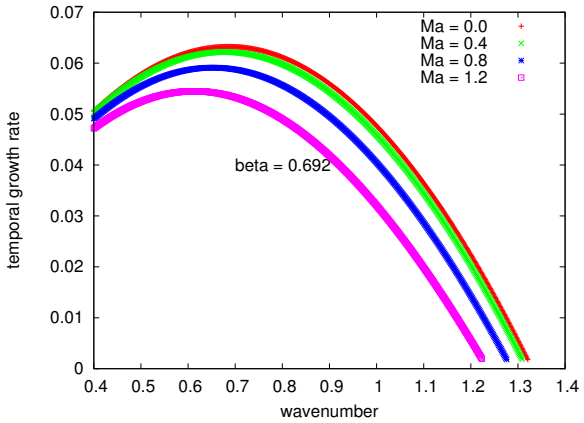

Figure 11. Wavenumber versus growth rate for $\beta = 0.692$

4. CONCLUSIONS

A local, normal modes stability analysis was performed for a compressible flow composed by a jet and a wake, and a jet, a wake and a mixing layer. The base flow is representative of the flow found at the trailing edge of a gas turbine blade, where the jet simulate the effect of a cooling flow ejection at the trailing edge. The results show that the jet has a distabilizing effect on the wake, but a stabilizing effect on the wake/mixing layer base flow. The compressibility has a stabilizing effect as does three-dimensionality. Further investigations will be conducted to evaluate the effect of the jet temperature on the stability.

5. REFERENCES

Brown, G. L., and Roshko, A. 1974. On density effects and large structure in turbulent mixing layers. *Journal of Fluid Mechanics*, **64**, 775–781.

Caillol, P. 2009. Absolute and convective instabilities of an inviscid compressible mixing layer:Theory and applications. *Physics of Fluids*, **21**, 104101–1–104101–17.

Fedioun, Ivan, and Lardjane, Nicolas. 2005. Temporal linear stability analysis of three-dimensional compressible binary shear layers. *AIAA Journal*, **43**(1), 111–123.

Gennaro, E. M., and Medeiros, M. A. F. 2008. Numerical and Theoretical Investigation of the Asymmetry Effects in a Wake Profile. *In: Brazilian School of Transition and Turbulence*. ABCM.

Gropengiesser, H. 1970. *Study on the stability of boundary layers in compressible fluids*. Tech. rept. NASA TT F-12. National Aeronautics and Space Administration – NASA.

Ho, C. M., and Huerre, P. 1984. Perturbed Free Shear Layers. *Ann. Rev. of Fluid Mechanics*, **16**, 365–424.

King, P. S., and Schetz, J. A. 1996. Interaction of jets and shear layers to produce instabilities and mixing enhancement in supersonic flows. *In: 34th AIAA Aerospace Sciences Meeting and Exhibit*. AIAA paper 96-0915.

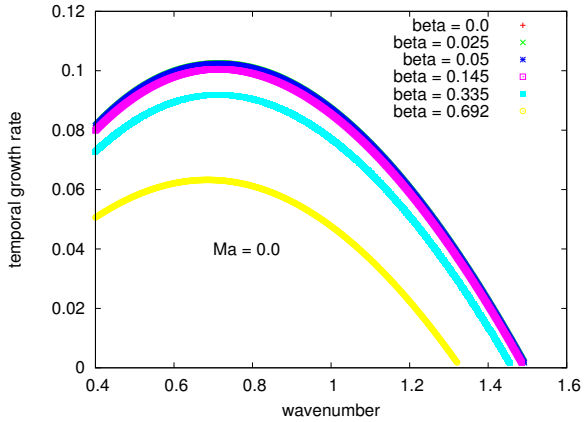

Figure 12. Wavenumber versus growth rate for $Ma = 0.0$

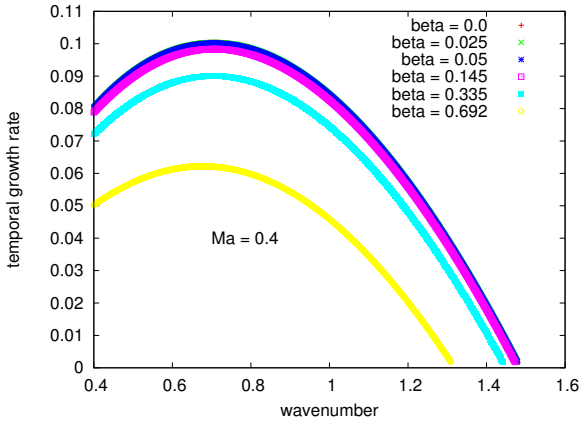

Figure 13. Wavenumber versus growth rate for $Ma = 0.4$

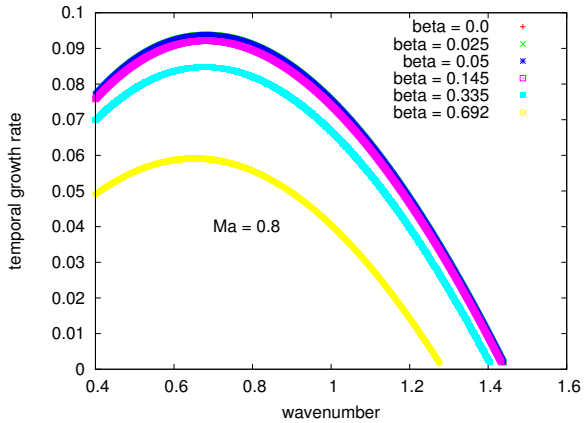

Figure 14. Wavenumber versus growth rate for $Ma = 0.8$

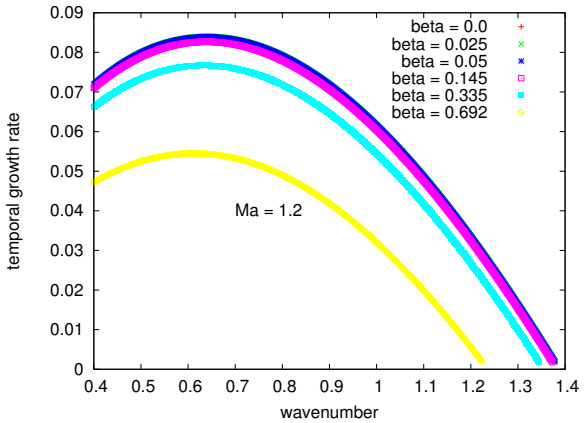

Figure 15. Wavenumber versus growth rate for $Ma = 1.2$

Salemi, L., and Mendonca, M. T. 2008. Spatial and Temporal Linear Stability Analysis of Binary Compressible Shear Layer. *In: AIAA 38th Fluid Dynamics Conference*. AIAA paper 2008-3841.

White, F. M. 1974. *Viscous Fluid Flow*. McGraw-Hill.

Winant, C. D., and Browand, F. K. 1974. Vortex pairing: the mechanism of turbulent mixing layer growth. *Journal of Fluid Mechanics*, **63**, 237–255.

Zhuang, M., and Dimotakis, P. E. 1995. Instability of wake-dominated compressible mixing layers. *Physics of Fluids*, **10**, 2489–2495.

6. Responsibility notice

The author is the only responsible for the printed material included in this paper

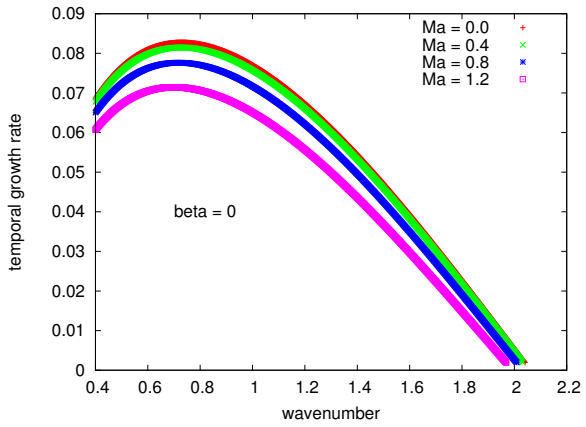

Figure 16. Wavenumber versus growth rate for $\beta = 0.0$

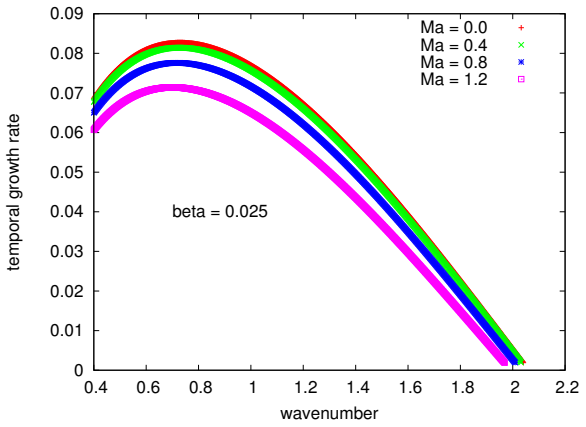

Figure 17. Wavenumber versus growth rate for $\beta = 0.025$

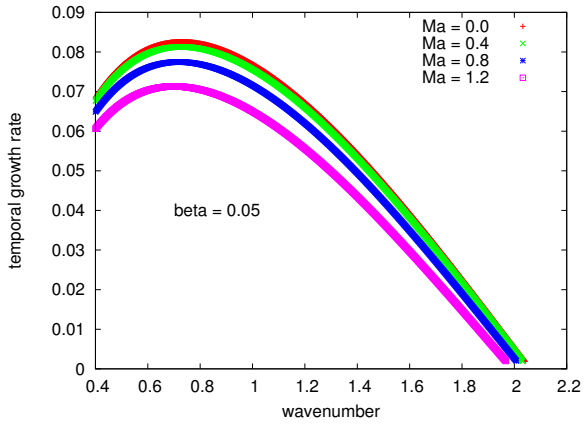

Figure 18. Wavenumber versus growth rate for $\beta = 0.05$

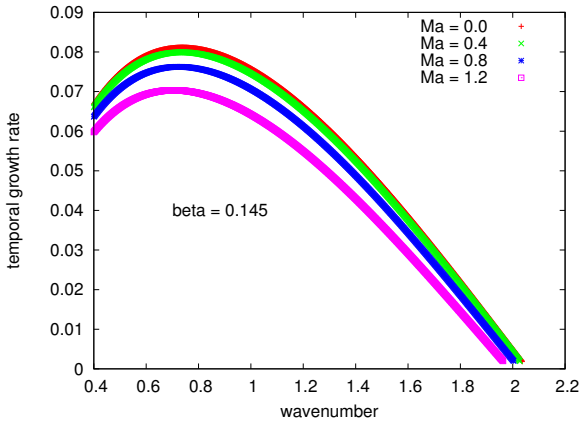

Figure 19. Wavenumber versus growth rate for $\beta = 0.145$

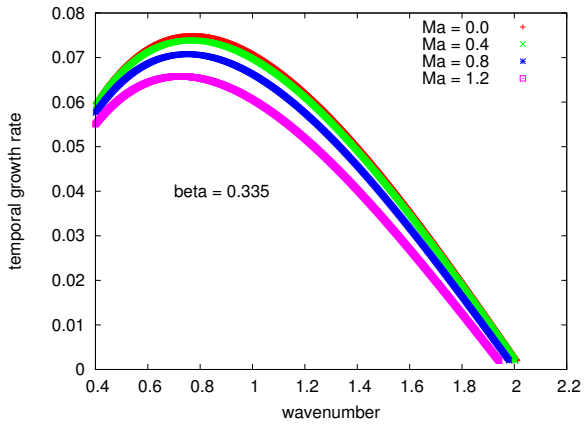

Figure 20. Wavenumber versus growth rate for $\beta = 0.335$

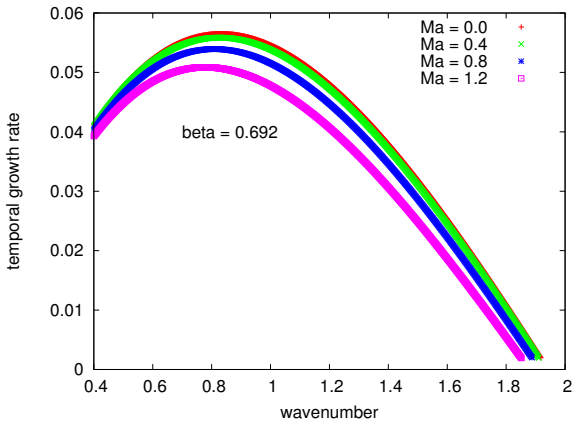

Figure 21. Wavenumber versus growth rate for $\beta = 0.692$

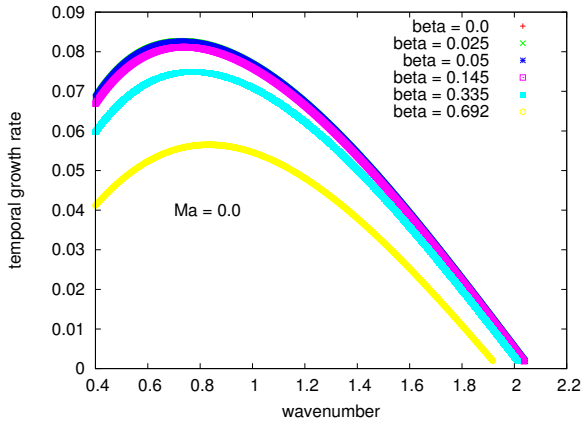

Figure 22. Wavenumber versus growth rate for $Ma = 0.0$

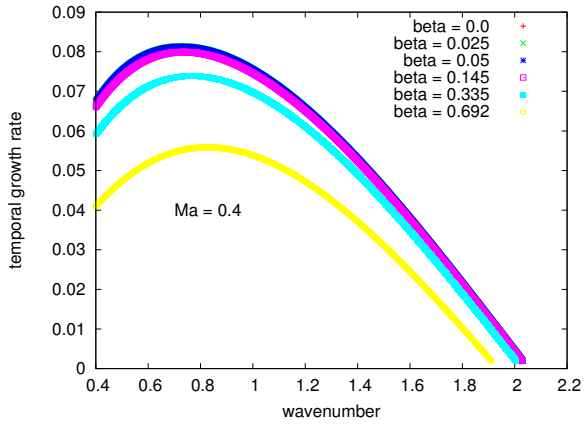

Figure 23. Wavenumber versus growth rate for $Ma = 0.4$

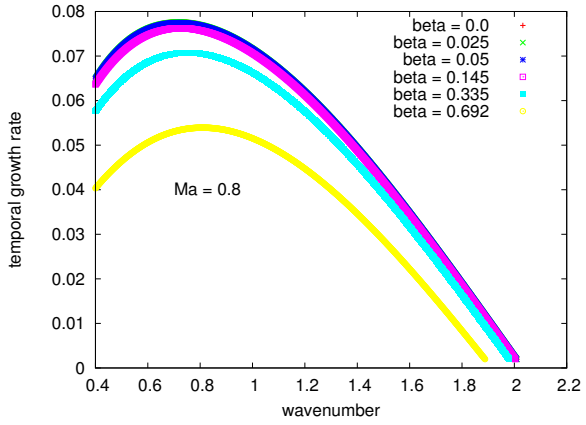

Figure 24. Wavenumber versus growth rate for $Ma = 0.8$

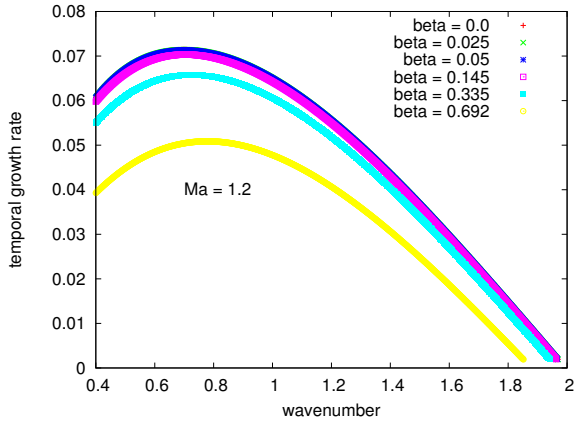

Figure 25. Wavenumber versus growth rate for $Ma = 1.2$

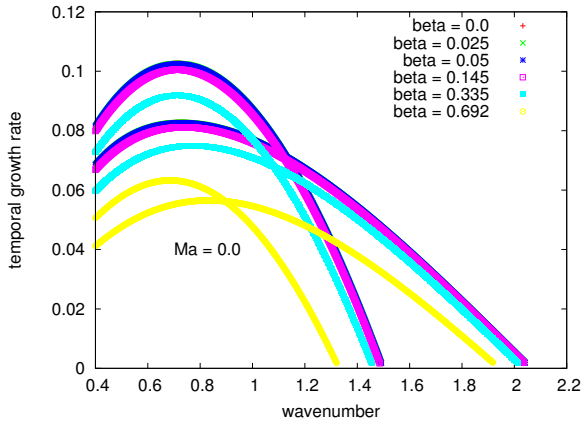

Figure 26. Wavenumber versus growth rate for $Ma = 0.0$, comparison between the wake/mixing layer profile with and without jet

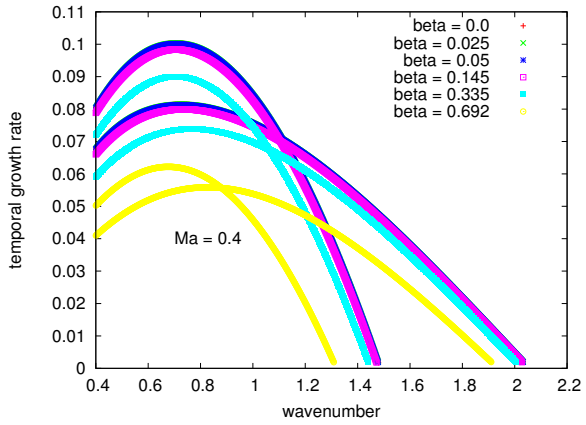

Figure 27. Wavenumber versus growth rate for $Ma = 0.4$, comparison between the wake/mixing layer profile with and without jet

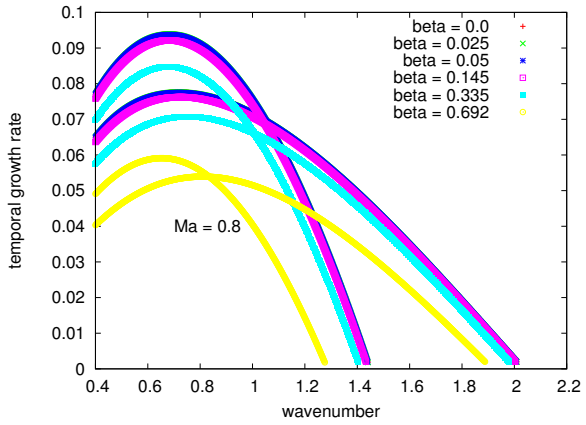

Figure 28. Wavenumber versus growth rate for $Ma = 0.8$, comparison between the wake/mixing layer profile with and without jet

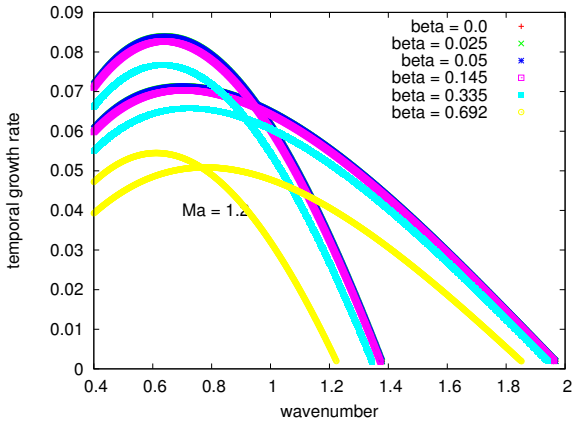

Figure 29. Wavenumber versus growth rate for $Ma = 1.2$, comparison between the wake/mixing layer profile with and without jet

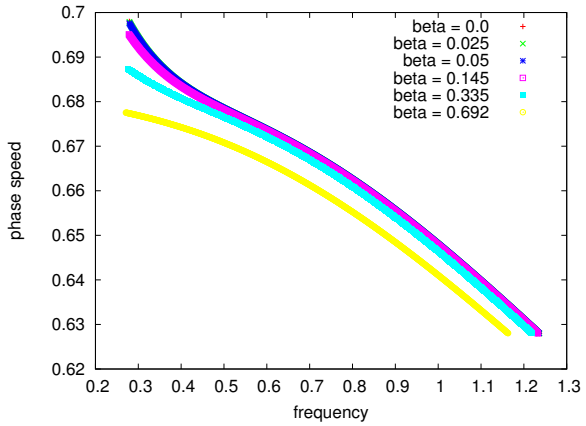

Figure 30. Wave speed versus frequency for different β at $Ma = 1.2$.

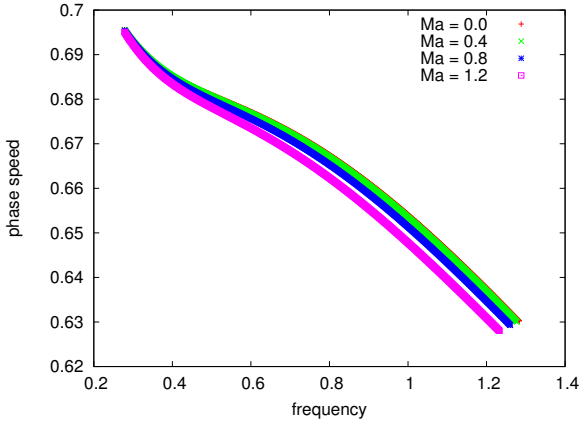

Figure 31. Wave speed versus frequency for different Ma at $\beta = 0.145$.